Reconstruction of the Pt(111) Surface

A. R. Sandy and S. G. J. Mochrie
Department of Physics, Massachusetts Institute of Technology, Cambridge, Massachusetts 02139-4307

D. M. Zehner
Solid State Division, Oak Ridge National Laboratory, Oak Ridge, Tennessee 37831-6057

G. Grübel, K. G. Huang, and Doon Gibbs
Department of Physics, Brookhaven National Laboratory, Upton, New York 11973-5000
(Received 22 July 1991)

The structure of the clean Pt(111) surface has been studied between 300 K and $0.92T_m$ ($T_m = 2045$ K) via x-ray scattering. The surface is unreconstructed for temperatures less than $0.65T_m$, but reconstructs at higher temperatures to form a layer isotropically compressed and incommensurate with the underlying bulk (111) planes. A disordered arrangement of discommensurations separates regions with ideal fcc stacking from regions with faulted stacking. With increasing temperature both the compression of the surface layer and the orientational order of the discommensurations increase.

PACS numbers: 68.35.Rh, 61.10.Lx, 64.70.Kb

A simple idea underlies our understanding of the reconstruction of many metal surfaces. Surface atoms have fewer nearest neighbors than atoms in the bulk. As a result, the surface energy may be reduced for an arrangement which leads to closer packing within the top layer. At the same time, such a reconstruction produces a misfit between the surface layer and the bulk, which increases the surface energy. The balance of these effects determines the surface structure. In the last several years, notable progress has been made along these lines in calculations of surface electronic structure which focus on the role of surface stress [1]. Moreover, this picture seems consistent with the reconstructions of the (001) surfaces of Ir [2], Au [3], and Pt [4], where hexagonal monolayers form on top of the substrate planes of square symmetry, with an atomic density which is 8% larger than that of the close-packed (111) planes of the bulk. Similarly, the Au(111) surface reconstructs to form a denser layer at room temperature [5,6]. Interestingly, the Au(111) surface compresses even further at higher temperatures [6]. This suggests that bonding to the substrate is effectively weakened at higher temperatures [7] and raises an interesting question: Might other metal surfaces, unreconstructed at lower temperatures, also undergo reconstructions at elevated temperatures? This question motivated the present work: an x-ray scattering study of the thermal behavior of the Pt(111) surface.

We find that Pt(111) is unreconstructed for temperatures less than 0.65 of the bulk melting temperature (T_m), consistent with earlier work [8]. However, our x-ray measurements reveal that above $0.65T_m$ the surface undergoes a continuous commensurate-incommensurate transformation [7] into a structure which is isotropically compressed relative to the (111) planes of the bulk. The reconstructed surface layer is composed of ideal stacking regions and faulted stacking regions. Separating these commensurate sublattices are discommensurations (incorporating extra surface atoms). A similar structure has been observed at temperatures above $0.65T_m$ for Au(111) [6]. Because the arrangement of discommensurations on Pt(111) is translationally disordered, we call the reconstructed phase a discommensuration fluid [9,10]. Near the transformation the discommensurations appear to be orientationally disordered as well. However, with increasing temperature, the mean separation between discommensurations decreases and sixfold orientational ordering of the discommensurations develops [11]. This paper presents the highlights of our results. A complete account is given in Ref. [12].

We studied a (111)-oriented disk of Pt [$< 0.006°$ mosaic full width at half maximum (FWHM)]. X-ray glancing-incidence and reflectivity measurements were made at beam lines X22C and X20A, respectively, at the National Synchrotron Light Source. At X22C, the sample was supported in an ultrahigh-vacuum chamber [3] with standard surface diagnostics. With a Ge(111) analyzer, we achieved a radial resolution of 0.001 Å^{-1} FWHM and a transverse resolution of 0.0003 Å^{-1} FWHM. At X20A, reflectivity measurements were made with the sample held in a vacuum chamber [6] mounted on a standard diffractometer. Slits defined both the illuminated sample area and the spectrometer resolution [6]. Surface preparation followed the procedures of Ref. [4]. We use a hexagonal coordinate system [6] to index reciprocal space. The H and K directions lie within the surface plane, as illustrated in the upper panel of Fig. 1. Within the H-K plane the unit of wave vector is $a^* = 4\pi/(\sqrt{3}a)$, where a is the bulk nearest-neighbor distance; along the surface normal (L direction), it is $c^* = 2\pi/(3d)$, where d is the separation between (111) planes in the bulk. ($a^* = 2.61$ Å^{-1} and $c^* = 0.92$ Å^{-1} at 300 K.)

Figures 1(a)–1(e) show a series of radial scans obtained along the K direction at different temperatures. In each case, there is a narrow peak (0.001 Å^{-1} FWHM) at $K = 1$, suggesting that at all temperatures the surface

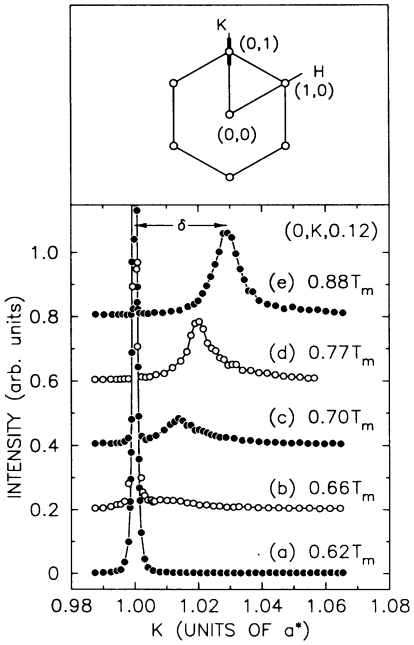

FIG. 1. Radial scans through the (0,1) truncation rod [13] vs temperature. Broad peaks at $K > 1$ are scattering from the temperature-induced surface reconstruction. Solid lines are guides to the eye. The top panel is a schematic of reciprocal space: The heavy line is the scan path.

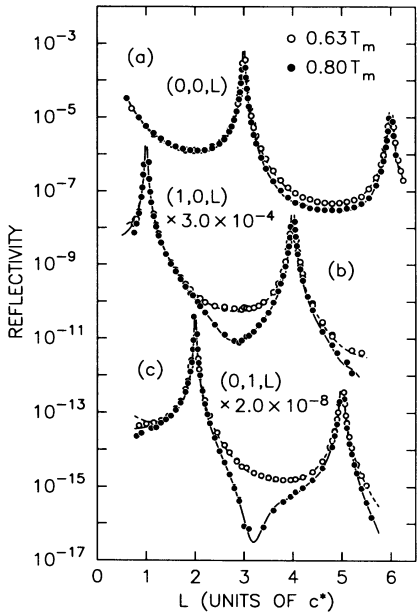

FIG. 2. Reflectivity profiles along (a) (0,0,L), (b) (1,0,L), and (c) (0,1,L) rods. Open circles are data obtained at $0.63T_m$ (unreconstructed surface) and solid circles are data obtained at $0.80T_m$ (reconstructed surface). Dashed and solid lines are the results of fits described in the text.

is smooth on a length scale exceeding 5000 Å [4]. Figure 1(a) is representative of data obtained at temperatures less than $0.65T_m$. Aside from the peak at $K=1$, no other scattering is evident, indicating that the surface is unreconstructed below $0.65T_m$. For temperatures immediately above $0.65T_m$ [Fig. 1(b)], a weak shoulder of scattering appears at $K > 1$. At higher temperatures [Figs. 1(c)–1(e)], the shoulder evolves into a distinct peak, separated from the truncation rod by an incommensurate wave vector (δ); the new peak corresponds to scattering from a temperature-induced, incommensurate reconstruction of the Pt(111) surface. The concentration of intensity at $K=1+\delta$ shows that, on-average, the surface layer is compressed within the surface plane relative to the bulk (111) planes. It may be seen in Figs. 1(c)–1(e) that δ increases continuously with increasing temperature, signaling a further compression of the surface layer and an accompanying decrease in the dimensions of the surface unit cell [$(4\pi/\sqrt{3})\delta = 100$–$350$ Å]. The radial widths of the reconstruction peaks change little above $0.71T_m$ and are about 0.02 Å^{-1} FWHM, from which we deduce a translational correlation length within the reconstructed layer of only 100 Å. Results shown in Fig. 1 and additional measurements [see Fig. 4(a)] demonstrate that the transformation is reversible and continuous.

To determine the microscopic character of the surface, we have performed measurements of the specular and nonspecular x-ray reflectivities [3,6] at $0.63T_m$ (open circles) and $0.80T_m$ (solid circles). Figure 2(a) displays the specular reflectivity [(0,0,L)], and Figs. 2(b) and 2(c) the nonspecular reflectivities along (1,0,L), and (0,1,L) respectively. Divergences at (0,0,3), (0,0,6), (1,0,1), (1,0,4), (0,1,2), and (0,1,5) correspond to bulk Bragg reflections. At $0.63T_m$, the smooth variations in reflectivity between the Bragg reflections are characteristic of an unreconstructed crystal. The specular reflectivity obtained at $0.80T_m$ is similar to that measured at $0.63T_m$ —the slight reduction in intensity between Bragg reflections may be accounted for by an increase in the amplitude of thermal vibrations at higher temperature. In contrast, the nonspecular reflectivities at the higher temperature are strikingly different from their counterparts at the lower temperature. The reflectivity profiles observed for Pt(111) at $0.80T_m$ are similar to the corresponding profiles observed for the (111) surface of Au [6], which were modeled by allowing surface atoms to occupy both ideally terminated fcc C-stacking sites and faulted A-stacking sites. The reflectivities of Pt(111) have been analyzed with a model for the reconstructed surface monolayer that allows a fractional occupancy of the C- (f_C) and A-stacking (f_A) sites and includes a possible increase in the density within the surface layer. In addition, the different stacking sites are located at different distances, d_C and d_A, respectively, above the second, unreconstructed layer. Finally, we allowed for increased amplitudes of atomic vibrations (as compared to in the bulk) along the surface-normal direction in the surface selvage. The best

fits are shown as dashed ($0.63T_m$) and solid ($0.80T_m$) lines in Fig. 2. They provide an excellent description of the measured reflectivities and confirm that a single layer is involved in the reconstruction. At $0.63T_m$, the fit is consistent with an unreconstructed surface. For $0.80T_m$, the best fit is obtained with $f_C = 0.70 \pm 0.03$ and $f_A = 0.18 \pm 0.03$. We infer that the remaining atoms lie between the C and A sites, forming discommensurations. Based on the discussion of Fig. 1, the arrangement of discommensurations is disordered with a correlation length within the reconstructed layer which is comparable to the unit cell size. We therefore call the reconstructed phase a discommensuration fluid [6,9,10]. The fits further suggest that atoms at faulted A sites are located farther from the second layer than atoms at unfaulted C sites, $d_A/d = 1.04 \pm 0.03$ and $d_C/d = 1.01 \pm 0.01$, that there is a slight enhancement of surface-normal vibrational amplitudes, and that the density of the surface layer increases slightly with temperatures increasing above $0.65T_m$.

Our discussion of the in-plane diffraction pattern has so far been limited to the results of one-dimensional scans along the K direction in reciprocal space (Fig. 1). However, a remarkable property of the scattering function within the discommensuration-fluid phase is its two-dimensional character. Measurements of the scattered intensity within the H-K plane show that above $0.65T_m$ the scattering function forms a cylinder about each truncation rod [14,15], as illustrated in the top panel of Fig. 3. The cylinder radius is δ. To characterize the temperature dependence of the scattering function we have performed "ring scans," which follow the peak of the scattering function around a circular path. Scattered intensities obtained at three temperatures within the discommensuration-fluid phase are shown in Figs. 3(a)–3(c). At $0.73T_m$ [Fig. 3(a)], the intensity is a maximum at $\theta = 0°$ $[(0,1+\delta)]$ and a minimum at $|\theta| = 180°$ $[(0,1-\delta)]$. Ring scans obtained at higher temperatures and, consequently, larger incommensurabilities (δ) are shown in Figs. 3(b) and 3(c). Like the scan obtained at $0.73T_m$, these scans have intensity maxima at $\theta = 0°$ and exhibit an overall decrease in intensity at larger $|\theta|$, which results from the net compression of the surface layer. However, the intensity also displays a clear sixfold angular modulation, the amplitude of which appears to increase with increasing temperature. To quantify the temperature dependence, we have fitted the ring scans by the expression

$$I(\theta) = [A + B\exp(-|\theta|^2/2\sigma^2)][1 + A_{6\theta}\cos(6\theta)] . \quad (1)$$

The first factor is an empirical form which reproduces the intensity variation due to the compression of the surface

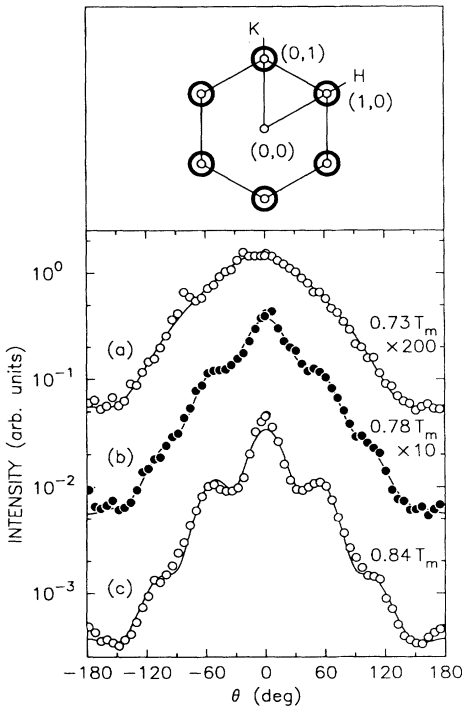

FIG. 3. "Ring scans" at (a) $0.73T_m$, (b) $0.78T_m$, and (c) $0.84T_m$. Solid lines are fits by Eq. (1). The top panel illustrates the diffraction pattern above $0.65T_m$.

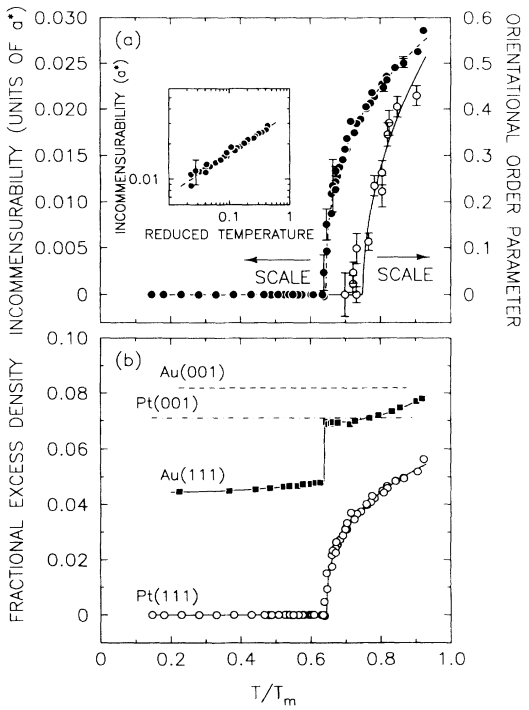

FIG. 4. (a) The orientational order parameter (open circles) and the incommensurability (solid circles) vs temperature. Fits to determine the incommensurability (and the error bars) are described in Ref. [12]. The dashed line is a best fit by the form $\delta = \delta_0 t^\lambda$, with $\delta_0 = (0.037 \pm 0.002)a^*$ and $\lambda = 0.35 \pm 0.04$. Inset: The behavior on a log-log scale. (b) Fractional excess densities of the (001) and (111) surfaces of Pt [4] and Au [3,6] vs temperature. Solid lines in (a) and (b) are guides to the eye.

layer [solid line in Fig. 3(a)]. The second term allows for a sixfold modulation. The best fits provide an adequate description of the data [solid lines in Figs. 3(a)–3(c)]. The corresponding reversible temperature dependence of $A_{6\theta}$ is shown in Fig. 4(a) (open circles), together with that of the incommensurability (solid circles). We believe that the appearance of the sixfold modulation about the ring results from an orientational ordering of the discommensurations as they pack more closely together. Thus, we are led to the following description of the phase behavior of Pt(111). Pt(111) is unreconstructed below $0.65T_m$. Between $0.65T_m$ and $0.75T_m$, the surface layer forms a translationally and orientationally disordered discommensuration fluid. Above $0.75T_m$, orientational order appears and grows continuously with further increase in the temperature [11]. Throughout the discommensuration-fluid phase, the incommensurability increases according to a $\frac{1}{3}$ power law versus reduced temperature [$t \equiv (T - 0.65T_m)/0.65T_m$], as shown by the dashed line in Fig. 4(a). Similar behavior is observed for Kr adsorbed on graphite [9]. There is not, at present, a satisfactory theory of this behavior in either case. In contrast, for a uniaxial system, the incommensurability is expected to follow a $\frac{1}{2}$ power law [7].

More generally, our data support the notion that metal surface reconstruction is driven by the relief of surface stress [1]. Figure 4(b) displays the fractional excess densities of the (001) and (111) surfaces of Pt and Au, as determined by the lattice constants of the surface layer [6], compared to the density of the close-packed bulk (111) planes. Temperatures are expressed as a fraction of the appropriate bulk melting temperatures ($T_m = 1337$ K for Au). Below $0.65T_m$, the density of the Pt(111) surface (open circles) is the same as that of the bulk (111) planes. Above $0.65T_m$, its excess density increases continuously with increasing temperature. A possible explanation of this behavior may be that the bonding to the substrate is effectively weaker at higher temperatures due to increased thermal vibrations [7]. As a result, the decrease in free energy accompanying a more closely packed surface is greater than the increase which arises because of the misfit between the surface layer and the substrate. Likewise, the (111) surface of Au becomes denser with increasing temperature (solid squares) [6]. Because of the markedly different bulk melting temperatures of Pt and Au, it is noteworthy that both the Pt(111) and Au(111) surfaces undergo a transformation into a structurally similar discommensuration-fluid phase at $0.65T_m$. However, in view of the similar phase behaviors of the reconstructed Pt(001) [4] and Au(001) [3] surfaces, this observation cannot come as a surprise. Also shown in Fig. 4(b) are the excess densities of the Pt(001) (dot-dashed line) [4] and Au(001) (dashed line) [3] surface layers. Although their temperature dependence is weak, the excess densities of the (001) surfaces are large and similar to those of the (111) surfaces at the highest temperatures.

In summary, we have presented the results of an x-ray scattering study of the phase behavior of the Pt(111) surface. Pt(111) is unreconstructed below $0.65T_m$. At $0.65T_m$, the surface layer undergoes a continuous, commensurate-incommensurate transformation into a translationally and orientationally disordered discommensuration-fluid phase. For temperatures increasing above $0.75T_m$, sixfold orientational order of the discommensurations appears and increases.

We would like to thank G. Ownby for his invaluable assistance. Work performed at MIT is supported by the NSF (DMR-8806591), at ORNL by the DMS, DOE (DE-AC05-840R21400) with MMES, Inc., and at BNL by the DOE (DE-AC0276CH00016). X20A is supported by the NSF (DMR-8719217) and IBM.

[1] R. J. Needs and M. Mansfield, J. Phys. Condens. Matter **1**, 7555 (1989). See also B. W. Dodson, Phys. Rev. Lett. **60**, 2288 (1988); N. Takeuchi, C. T. Chan, and K. M. Ho, Phys. Rev. Lett. **63**, 1273 (1989).

[2] M. A. Van Hove, R. J. Koestner, P. C. Stair, J. P. Bibérian, L. L. Kesmodel, I. Bartos, and G. A. Somorjai, Surf. Sci. **103**, 189 (1981).

[3] S. G. J. Mochrie, D. M. Zehner, B. M. Ocko, and D. Gibbs, Phys. Rev. Lett. **64**, 2925 (1990); D. Gibbs, B. M. Ocko, D. M. Zehner, and S. G. J. Mochrie, Phys. Rev. B **42**, 7330 (1990); B. M. Ocko, D. Gibbs, K. G. Huang, D. M. Zehner, and S. G. J. Mochrie, Phys. Rev. B **44**, 6429 (1991).

[4] D. Gibbs, G. Grübel, D. M. Zehner, D. L. Abernathy, and S. G. J. Mochrie, Phys. Rev. Lett. **67**, 3117 (1991); D. L. Abernathy, S. G. J. Mochrie, D. M. Zehner, G. Grübel, and D. Gibbs, Phys. Rev. B (to be published).

[5] U. Harten, A. M. Lahee, J. P. Toennies, and Ch. Wöll, Phys. Rev. Lett. **54**, 2619 (1985).

[6] K. G. Huang, D. Gibbs, D. M. Zehner, A. R. Sandy, and S. G. J. Mochrie, Phys. Rev. Lett. **65**, 3313 (1990); A. R. Sandy, S. G. J. Mochrie, D. M. Zehner, K. G. Huang, and D. Gibbs, Phys. Rev. B **43**, 4667 (1991).

[7] See, for example, V. L. Pokrovsky and A. L. Talapov, *Theory of Incommensurate Crystals* (Harwood Academic, New York, 1984).

[8] For example, K. Christmann, G. Ertl, and T. Pignet, Surf. Sci. **54**, 365 (1976).

[9] D. E. Moncton, P. W. Stephens, R. J. Birgeneau, P. M. Horn, and G. S. Brown, Phys. Rev. Lett. **46**, 1533 (1981).

[10] S. N. Coppersmith, D. S. Fisher, B. I. Halperin, P. A. Lee, and W. F. Brinkman, Phys. Rev. B **25**, 349 (1982); J. Villain and P. Bak, J. Phys. (Paris) **42**, 657 (1981).

[11] D. R. Nelson and B. I. Halperin, Phys. Rev. B **19**, 2457 (1979).

[12] G. Grübel, K. G. Huang, D. Gibbs, D. M. Zehner, A. R. Sandy, and S. G. J. Mochrie (unpublished).

[13] I. K. Robinson, Phys. Rev. B **33**, 3830 (1986).

[14] G. Reiter and S. C. Moss, Phys. Rev. B **33**, 7209 (1986).

[15] F. Grey, R. Feidenhans'l, J. S. Pedersen, M. Nielsen, and R. L. Johnson, Phys. Rev. B **41**, 9519 (1990).